

AD-A127 562

EVOKED POTENTIAL STUDIES OF THE EFFECTS OF IMPACT
ACCELERATION ON THE MOTOR NERVOUS SYSTEM(U) TEXAS
RESEARCH INST OF MENTAL SCIENCES HOUSTON

1/1

UNCLASSIFIED

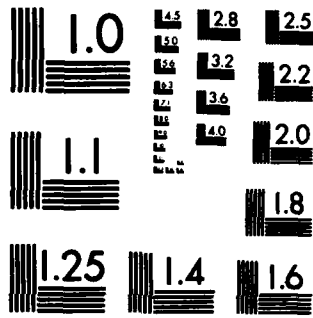
B SALTZBERG ET AL. 1983 N00014-76-C-0911

F/G 6/19

NL



END
DATE
FILMED
5 83
DTIC



MICROCOPY RESOLUTION TEST CHART
NATIONAL BUREAU OF STANDARDS-1963-A

EVOKED POTENTIAL STUDIES OF THE EFFECTS OF
IMPACT ACCELERATION ON THE MOTOR NERVOUS SYSTEM

B. Saltzberg¹, W.D. Burton Jr.¹, N.R. Burch¹, C.L. Ewing²,
D.J. Thomas², M.S. Weiss², M.D. Berger², A. Sances Jr.³,
P.R. Walsh³, J. Myklebust³, S.J. Larson³, E. Jessop²

¹Texas Research Institute of Mental Sciences, Houston, Texas

²Naval Biodynamics Laboratory, New Orleans, Louisiana

³Medical College of Wisconsin, Milwaukee, Wisconsin

AD A127002

12

DTIC
SELECTED
MAY 3 1968
H

ABSTRACT

The initial results of a continuing investigation into the effects of various levels of impact acceleration on the functional integrity of the motor nervous system are summarized. The results are based on the measurement of alterations in neural transmission along the motor pathway of the *Rhesus* monkey as revealed by latency and amplitude changes in the motor pathway evoked potential (EP) following the delivery of various levels of impact acceleration to a test vehicle. The EPs were produced by electrical stimulation of and recording from the motor pathway of experimental animals subjected to -Y (lateral impact) acceleration and animals subjected to -X (frontal impact) acceleration. High resolution latency and amplitude measures of the EP recorded from these animals before and after impact were tracked so that the time course of recovery of nerve propagation following impact could be accurately assessed. Analysis of these EP measures revealed that the time course of recovery to pre-impact values is directly related to the intensity of the acceleration impulse delivered to the test vehicle.

METHODS

-Y EXPERIMENT - Four *Rhesus* monkeys were subjected to a total of eight sled impact acceleration runs at NBDL to reproduce the dynamic forces which act on the head, and on the spinal column and cord in a lateral (-Y) collision. Each animal was subjected to a 10-G control impact, followed later the same day by a larger impact. The larger impacts were: 30-G for animal AR-8849, 50-G for animal AR-2152, 70-G for animal AR-8695, and 90-G for animal AR-8816. Analyses of only the 30, 50, 70, and 90-G runs are

presented here since the 10-G runs showed no significant post-impact EP changes.

Electrical stimulation was applied to the spinal cord with recording of evoked activity from the left and right sensorimotor cortex (CXL and CXR). Surgical procedures for electrode implantation were carried out under barbiturate anesthesia with endotracheal intubation and atropine premedication. Stimulating electrodes were a five-in-line lead parallel array placed over the spinal cord. Recording electrodes were placed over the left and right sensorimotor cortex. Details of the electrode configurations and surgical implantation procedures are described in Reference (1)*. All stimuli were constant current rectangular pulses of 0.2 millisecond duration. Current levels (approximately 1.25 milli-ampere) were applied sufficient to obtain good afferent evoked potentials.

Copies of the analog data tapes from the NBDL -Y impact experiments were processed at the Texas Research Institute of Mental Sciences (TRIMS) using Average Evoked Potential (AEP) analysis programs written specifically for this project. The analog data consisted of two channels of EEG data, a stimulus marker channel, and a time-code channel. These data constituted the input to a PDP-11 computer equipped with an AR-11 analog-to-digital converter (10-bit resolution). The time code was used to control the digitizing start and stop times relative to experimental impact. The stimulus marker controlled the start of data acquisition for individual responses. In order to achieve high resolution in measuring the latency of AEP components, the analog tape was slowed to half its normal speed, and appropriate adjustments were made to playback discriminators and the sampling interval. The final digitized data resolution was 25 microseconds per print (equivalent to 40,000 samples per second).

Starting on the rise of the stimulus mark pulse, 2000 digital samples were used to obtain AEPs of 50 milliseconds duration. Initially, *Numbers in parentheses designate references at end of paper.

*This work was supported by the Office of Naval Research contract #N00014-76-C-091.

This document has been approved for public release and sale; its distribution is unlimited.

8-8 05 02 11Z

B. Saltzberg, et. al.

5 individual responses were averaged to create each AEP. The AEPs were written to digital tape for subsequent processing. Preliminary examination of the AEPs (based on 5 responses) immediately following impact revealed a significantly noisy pattern and, therefore, additional averaging was necessary. However, to achieve good time resolution of temporal changes in amplitude and latency components of the AEPs, it was necessary to minimize (within the constraints of noise) the number of individual responses used to obtain a smooth AEP. Using AEPs consisting of 50 individual responses met both criteria in that the resulting improvement in signal-to-noise ratio gave a smooth AEP while providing a reasonably good time resolution of 10 seconds.

In order to visualize overall changes in AEP waveshape, compressed AEP plots were produced. These plots show the time course of AEPs over a period of 12 minutes, beginning 2 minutes prior to impact. Compressed AEP plots for the left and right cortical leads (CXL and CXR) from each of the 4 experiments are shown in Figures 1 through 4.

The feature most common to AEPs from the 4 different animals was a peak which occurred in the latency range from 9 to 13 milliseconds following the stimulus. Except in animal AR-2152, used for the 70-G run, this peak was positive-going, and will be referred to as E10. An AEP component in the latency range 15 to 20 milliseconds (designated E15) was found in all animals except AR-8816, the animal used for the 90-G experiment.

Quantification of changes in the AEPs was done by tracking the amplitude and latency of the E10 and, where possible, the E15 peaks. The mean and standard deviation of the measures were computed from 23 AEPs, starting 4 minutes prior to impact. These were used in comparing pre- and post-impact AEP measures. Changes were defined as significant when the measured value for 2 successive AEPs deviated by more than 1 standard deviation from the pre-impact mean. Recovery time for a measure was defined as the time from impact to the first value within 1 standard deviation of the pre-impact mean.

-X EXPERIMENT-A *Rhesus* monkey was subjected to a total of eight sled impact acceleration runs at the NBDL to reproduce the dynamic forces which act on the head, and on the spinal column and cord in a frontal (-X) collision. Electrical stimulation was applied to the sensorimotor cortex with recording of evoked activity from the thoracic spinal cord. Surgical procedures for electrode implantation were carried out under barbiturate anesthesia with endotracheal intubation and atropine premedication. Stimulating electrodes were a five-in-line lead parallel array placed over the motor cortex. Recording electrodes were placed over the lateral column of the thoracic spinal cord. All stimuli were constant current rectangular pulses of 0.2 millisecond duration. Current levels (approximately 3 milliamperes) were applied sufficient to obtain

good efferent evoked potentials. The digitized data resolution was 25 microseconds per point (equivalent to 40,000 samples per second).

A previous measurement of the actual stimulus rate indicated stimulus presentation at 191.5 stimuli per second; therefore, the inter-stimulus interval was slightly more than 5 milliseconds. Starting on the rise of the stimulus mark pulse, the subsequent 2.25 milliseconds (90 samples) were skipped because this interval contained a large electrical stimulus artifact. The following 110 digital samples were used to obtain AEPs of 2.75 milliseconds duration.

Initially, 20 individual responses were averaged to create each AEP. The AEPs were written to digital tape for subsequent processing. Preliminary examination of the AEPs (based on 20 responses) immediately following impact revealed a significantly noisy pattern and, therefore, additional averaging was necessary. However, to achieve high time resolution of temporal changes in amplitude and latency of components of the AEPs, it was necessary to minimize (within the constraints of noise) the number of individual responses used to obtain a smooth AEP. Using AEPs consisting of 100 individual responses met both criteria in that the resulting 10/1 improvement in signal-to-noise ratio gave a smooth AEP and a 0.52 second time resolution window. Figure 7 is a typical AEP, and it illustrates the evoked potential components that were tracked in this study. Two components of the AEP are clearly defined in this figure: a negative-going peak (N_1), which occurs at around 3 milliseconds after stimulus, and a positive-going peak (P) at about 3.4 milliseconds.

A simple program detected the most negative point of the AEP in the latency range 2.975 to 3.200 milliseconds (N_1) and the most positive point (P) between 3.400 to 4.000 milliseconds post-stimulus. Amplitudes were measured relative to the mean of the AEP determined from samples between 2.250 and 2.325 milliseconds.

Stimuli were applied during the time starting about 1 minute before test sled firing, and continued for a time interval between 1.5 and 5.0 minutes after firing, depending upon the run. The averaging and peak measuring procedure was repeated every 0.52 seconds during this time, yielding about 115 AEPs per minute over the course of the stimulation.

In order to visualize changes in AEP waveshape, plots similar to Figure 8 were generated. This figure shows the time course of changes in the AEP over a period of 1.2 minutes beginning 0.1 minutes pre-impact.

Accession For		<input checked="" type="checkbox"/> <input type="checkbox"/> <input type="checkbox"/>
NSIS OPAAI		
DTIC 2-8		
Unannounced		
Justification		
By		
Distribution/		
Availability Codes		
Dist	Avail and/or	
	Special	
A		B. Saltzberg, et. al.



RESULTS

-Y EXPERIMENT-Tables 1 through 4 summarize effects on the amplitude and latency of the E10 and E15 AEP components from the 4 acceleration levels studied. Listed in the tables are:

1. The percent relative deviation of the measure during 4 minutes pre-impact (standard deviation \div mean \times 100,
2. The maximum change post-impact, expressed as percent of the pre-impact mean, and
3. The recovery time

For those instances where the post-impact changes were not significant, the recovery time is reported as zero.

Table 1 shows the effects of impact on the amplitude of the E10 component. At 30-G, the amplitude is reduced in both the CXR and CXL leads. Following 50-G acceleration, the amplitude is reduced more in the right lead (76%) than in the left lead (70%). The 70-G impact produced an increase in the amplitude of the E10 peak on the left side, and a decrease on the right side.

The largest and most asymmetric effect on amplitude took place at 90-G acceleration, as shown in Figure 5. The amplitude of the left lead E10 component increases slightly for 30 seconds following impact, while the positive-going E10 component is completely obliterated from the right lead. This effect lasts for 4 minutes post-impact. Between 4 and 5.9 minutes, the amplitude recovers to nearly its pre-impact value before falling again. The amplitude leaves the recovery band again at 6.8 minutes and reaches a reduced stable value by 10 minutes post-impact. Between 10 and 58 minutes, the amplitude exhibits a very slow recovery trend. The amplitude variability from AEP to AEP is markedly less during this time than during the pre-impact period.

For all 4 acceleration levels, the E10 amplitude recovery time recorded from the right lead is considerably longer than for the left lead. Recovery in the left lead following 50-G impact is slightly longer than it takes at 30-G. The right lead at 50-G recovers in about half the time compared to 30-G. At the 70-G acceleration, the left lead required 5 minutes to recover, while the right lead had not recovered during the 6.5 minutes of post-impact data studied. Only 6.5 minutes for this run were used due to a technical problem which is now being corrected. Two recovery times are listed for the 90-G run, the first (5.8 minutes) represents the initial amplitude rebound; the second (58.6 minutes) is for long-term effect.

Table 2 is a summary of the latency changes for the E10 component of the AEP. There were no significant changes in latency associated with 30-G impact. At 50-G, the left lead component shows a 9.2% reduction in latency, while the right lead shows a 2.3% increase. The recovery time shown for the CXR lead of the 70-G run is

not a reliable estimate because of the small maximum change relative to the pre-impact variability.

The 90-G acceleration gives rise to the most asymmetric effect. As shown in Figure 6, the latency of the left cortical E10 component increases 7.9% following impact, and recovery takes place within 1 minute. The left pathway latency increases and decreases again between 4 and 8 minutes post-impact. This time corresponds to the time when the right cortical AEP amplitude is rebounding. After 8 minutes, the latency of the left E10 component reaches a mean value which is about 2% less than its pre-impact value.

By comparison, the right cortical E10 component of the AEP reappears at 4 minutes post-impact, and its latency is 12% greater than before impact. Latency recovery takes about 7.2 minutes post-impact, a time which also corresponds with the amplitude rebound of this component. From 7.2 minutes on, the latency appears to stabilize to a slightly smaller value than it had pre-impact. This is probably due to the double hump shape of the E10 component in this experiment (Figure 4). Prior to impact, the second hump was consistently larger and was the one detected as the extremal. Following impact, the first hump is larger and, therefore, was detected as the extremal.

Table 3 summarizes the changes in amplitude of the E15 component of the AEP. The higher variability in the measured amplitudes during pre-impact time makes interpretation of this data more difficult. The 30-G impact had the effect of increasing the amplitude in the CXL lead, but had no effect on the CXR lead. At 50-G and 70-G, the amplitude on both sides was reduced, as was the amplitude of the E15 component in the CXL lead of the 90-G experiment. The E15 component could not be reliably detected in the CXR lead of the 90-G experiment. In all runs, recovery of amplitude occurred within 1.7 minutes post-impact.

Table 4 shows that only in the 90-G run is there any effect on the latency of the E15 component of the AEP. The latency increased by 7%, and recovered in 40 seconds.

-X EXPERIMENT-In order to quantify the effect of -X impact, the amplitude and latency for both the N₁ and P components of the AEP were tracked as a function of time using the same procedures applied to the -Y data. Figures 9 through 24 are tracking plots of these measures for runs covering impacts in the -X direction at 20, 60, 80, and 100-G. The horizontal line through the pre-impact data represents the mean of the measure computed over a 30-second interval (57 AEPs) immediately preceding impact.

Latency Effects-Figure 9 shows the effect of impact at 100-G on the latency of the N₁ component of the AEP. The latency immediately following impact is difficult to determine because the amplitude during this time is virtually zero (see Figure 17). As the amplitude

begins to recover (about 10 seconds after impact), the latency has increased from its pre-impact mean, 2.9 milliseconds, to 3.3 milliseconds. The latency returns toward its pre-impact level until approximately 2 minutes post-impact, when it stabilizes to a constant value of 3.1 milliseconds. This vanishing of variability in response latency persists to the end of stimulation at 5 minutes post-impact.

The effect at 80-G on N_1 latency is illustrated in Figure 12. The time course of recovery is similar to that seen at 100-G, with the same transient increase followed by a gradual return to a stable level which is larger than the pre-impact latency. It should be noted that at 80-G the post-impact latency is more variable than at 100-G.

In contrast to the 100-G and 80-G runs, there was no slow transient latency change following impact at 60-G (Figure 9). Instead, the latency increased abruptly from 2.980 milliseconds pre-impact to 3.000 milliseconds post-impact (see Figure 11). This latency shift remains until the end of stimulation. There is a transient change at 2.2 minutes post-impact, but the 25-microsecond latency resolution is insufficient to track its time course in detail.

There is only a slight increase in latency (equivalent to about one sample interval) following 20-G impact (see Figure 10). However, this slight increase persisted to the end of stimulation.

The effect of impact on the latency of the positive-going (P) component of the AEP is shown in Figures 13 through 16. The effect follows the same pattern as seen for the N_1 component, although there is greater variability in the post-impact latency for the 100-G run.

Amplitude Effects-The effect of 100-G impact on the amplitude of the N_1 component of the AEP is shown in Figure 17 which reveals that immediately after impact the amplitude of N_1 drops to zero for about 10 seconds. It returns to its pre-impact level about 45 seconds after impact and then overshoots about 10 percent beyond its pre-impact value and remains at this higher level for the rest of the stimulus period. This overshoot effect is probably due to a reduction in latency variability of the N_1 component (shown in Figure 9) during this time, since a reduction in latency variability affects averaging in a way consistent with this observed result.

At 30-G (Figure 18), the amplitude of the N_1 component is reduced to about one-third of its pre-impact value. It gradually recovers and returns to its pre-impact value by 1.8 minutes post-impact. It should also be noted that throughout the post-impact period, the amplitude is less variable than during the pre-impact period.

The 60-G run (Figure 19) shows little effect on N_1 amplitude following impact. The amplitude is reduced slightly but soon recovers to its pre-impact mean value, but with significantly

increased variability. At about 2.2 minutes post-impact, the overall N_1 amplitude is reduced by about 20 percent. The time of this reduction corresponds to the time when the latency has increased, as shown in the N_1 latency profile in Figure 11.

At 20-G, there is no significant effect on the amplitude of the N_1 component (Figure 20).

At the 4 impact levels used in these experiments, the amplitude of the positive-going (P) component of the AEP was affected in a manner similar to the N_1 component amplitude with the following exceptions. At 100-G (Figure 21), the P component amplitude did not show the overshoot apparent in the N_1 amplitude at 100-G. This is due to the greater variability in latency of the P component as compared to the latency of the N_1 component which is evident in these figures.

At 80-G (Figure 22), the P amplitude does not recover to its pre-impact mean level by the end of the stimulus period (2.5 minutes). The amplitude is reduced following impact and slowly returns toward the baseline level. During the post-impact period, the amplitude variability is also reduced.

At 60-G (Figure 23), the amplitude of the P component is reduced slightly following impact, and persists until 2.2 minutes after impact when the amplitude is further reduced.

At 20-G (Figure 24), there is virtually no change in the amplitude of the P component.

SUMMARY OF FINDINGS AND CONCLUSIONS

-Y EXPERIMENT-Inssofar as lateral impact acceleration is concerned, the evoked potential data produced in the NBDL experiment reported here indicates that neural propagation from the spinal cord to the sensorimotor cortex is more severely altered along the right pathway than along the left pathway. The analysis presented has been limited to an examination of only two components of the EP, a component of approximately 10 milliseconds latency and a component at approximately 15 milliseconds latency. There are other less prominent components in the range from 7 to 20 milliseconds which have not been analyzed as yet, as well as late components which may have neurophysiological significance with regard to understanding the effects of impact acceleration on the motor nervous system. The early components in particular may offer some interesting insights on how brainstem activity is affected.

The -Y findings to date indicate that at all 4 acceleration levels, the E10 amplitude of the right cortical response takes longer to recover than the left cortical response. At the 70-G and 90-G acceleration levels, there is a long-term effect on the E10 amplitude which was not present at lower impact levels. At the 90-G level, the E10 component was obliterated from the right cortex lead for 4 minutes post-impact.

The recovery time of E15 amplitude varied directly with impact intensity, while E15 latency was only slightly affected by impact intensity.

-X EXPERIMENT-Significant transient and steady state changes in the efferent EP following -X impact were present. These changes are especially apparent in latency of the N₁ component of the AEPs. The short-term transient effects are present at impact levels of 80 and 100-G, and consist of a reduction in amplitude and an increase in latency of both the N₁ and P evoked potential components. These parameters return to steady state values within 2 minutes following impact. At the 20 and 60-G impact levels, the post-impact effects on the AEP are dominated by steady state changes in N₁ and P components. Increases in latency persist for the duration of the stimulus period in each run. When stimulation was restarted in preparation for the next acceleration run, it was noted that the latency had returned to nearly its previous pre-run value and, therefore, recovery occurred sometime after the recording was stopped between runs.

Although the magnitude of the latency shift is small for the lower G levels, the change is statistically significant because the latency variability from average to average is small compared to the latency shift. The average latency for 30 seconds immediately pre-impact was computed from 58 AEPs and compared to the average latency computed from an equivalent data sample post-impact. The change in average latency pre-versus post-impact was statistically significant ($p < 0.0005$), using a one-tailed student's T or

Kolmogorov-Smirnov test for equality of means. The mean latency change and latency variability following different impact levels are summarized in Table 5. From this table it can be seen that latency of the N₁ and P components of the EP increase with increasing impact G level. Average latencies of the N₁ component for the 20 and 60-G runs were approximately of the same magnitude and are the only exceptions to increasing latency with increasing G level. Although amplitude changes in the individual EPs do occur, average amplitude could not be reliably correlated with impact G level because these averages are significantly affected when large latency variability of the individual EPs occur and, therefore, average amplitude is not an appropriate measure under these conditions.

REFERENCES

Walsh, P.R., Larson, S.J., Sances, A., Jr., Ewing, C.L., Thomas, D.J., Weiss, M., Berger, M., Myklebust, J., Cusick, J.F., and Saltzberg, B. Experimental methods for evaluating spinal cord injury during impact acceleration. In Electrotherapeutic Sleep and Electroanesthesia, Vol. V, F.M. Wageneder and R.H. Germann, Eds., Universitat Graz, 1978, pp. 55-58.

TABLE 1
SUMMARY OF CHANGES IN AMPLITUDE OF E10 COMPONENT

<u>RUN</u>	<u>MEASURE</u>	<u>CXL-LEFT LEAD</u>	<u>CXR-RIGHT LEAD</u>
30-G pre-impact	relative amplitude deviation	7.5%	6.6%
	Maximum change	-29.8%	-28.8%
	Recovery time	52 seconds	208 seconds
50-G pre-impact	relative amplitude deviation	15.9%	16.7%
	Maximum change	-69.8%	-75.9%
	Recovery time	69 seconds	100 seconds
70-G pre-impact	relative amplitude deviation	33.8%	23.0%
	Maximum change	55.9%	-52.0%
	Recovery time	300 seconds	390 seconds (Note 1)
90-G pre-impact	relative amplitude deviation	20.2%	15.5%
	Maximum change	29.9%	100.0% (Note 2)
	Recovery time	30 seconds	356 seconds (5.9 minutes) (Note 3)
			3518 seconds (58.6 minutes)

NOTES

1. Data for only 6.5 minutes post-impact was tracked for the 70-G run. Recovery had not taken place by that time.
2. The positive E10 component was completely eliminated for 4 minutes post-impact.
3. After the 90-G impact, the amplitude recovered, then fell to a lower, slowly recovering value (see text).

Saltzberg, Etal.

TABLE 2

SUMMARY OF CHANGES IN LATENCY OF E10 COMPONENT

<u>RUN</u>	<u>MEASURE</u>	<u>CXL-LEFT LEAD</u>	<u>CXR-RIGHT LEAD</u>
30-G	pre-impact relative latency deviation	1.8%	1.0%
	Maximum change	NS	NS
	Recovery time	0	0
50-G	pre-impact relative latency deviation	2.2%	0.5%
	Maximum change	-9.2%	2.3%
	Recovery time	27 seconds	79 seconds
70-G	pre-impact relative latency deviation	0.5%	2.7%
	Maximum change	2.2%	4.4%
	Recovery time	94 seconds	21 seconds
90-G	pre-impact relative latency deviation	1.9%	1.6%
	Maximum change	7.9%	12.0%
	Recovery time	50 seconds	430 seconds

TABLE 3

SUMMARY OF CHANGES IN AMPLITUDE OF E15 COMPONENT

<u>RUN</u>	<u>MEASURE</u>	<u>CXL-LEFT LEAD</u>	<u>CXR-RIGHT LEAD</u>
30-G	pre-impact relative amplitude deviation	47.7%	65.7%
	Maximum change	119.5%	NS
	Recovery time	41 seconds	0
50-G	pre-impact relative amplitude deviation	.24.6%	54.7%
	Maximum change	-78.7%	-100.0%
	Recovery time	100 seconds	69 seconds
70-G	pre-impact relative amplitude deviation	31.4%	20.4%
	Maximum change	-99.4%	-74.0%
	Recovery time	94 seconds	94 seconds
90-G	pre-impact relative amplitude deviation	30.0%	Note 1
	Maximum change	-69.0%	
	Recovery time	60 seconds	

NOTE

1. The E15 component could not be reliably tracked in the 90-G run.

TABLE 4

SUMMARY OF CHANGES IN LATENCY OF E15 COMPONENT

<u>RUN</u>	<u>MEASURE</u>	<u>CXL-LEFT</u>	<u>CXR-RIGHT LEAD</u>
30-G	pre-impact relative latency deviation	1.8%	2.3%
	Maximum change	NS	NS
	Recovery time	0	0
50-G	pre-impact relative latency deviation	1.7%	1.9%
	Maximum change	NS	NS
	Recovery time	0	0
70-G	pre-impact relative latency deviation	0.7%	0.6%
	Maximum change	NS	NS
	Recovery time	0	0
90-G	pre-impact relative latency deviation	2.9%	Note 1
	Maximum change	7.1%	
	Recovery time	40 seconds	

NOTE

1. The E 15 component could not be reliably tracked in the 90-G run.

TABLE 5

COMPARISON OF EFFERENT AEP LATENCY

N₁ LATENCY

<u>-X</u> <u>IMPACT</u> <u>LEVEL</u>	<u>PRE-IMPACT</u>		<u>POST-IMPACT</u>		$\mu_2 - \mu_1$	<u>SIGNIFICANCE</u>
	μ_1	σ_1	μ_2	σ_2		
20 G	3.053	0.008	3.080	0.013	0.027	p<0.0005
60 G	2.977	0.006	3.002	0.006	0.025	p<0.0005
80 G	3.005	0.010	3.042	0.012	0.037	p<0.0005
100 G	3.001	0.019	3.075	0.000	0.074	p<0.0005

P LATENCY

<u>-X</u> <u>IMPACT</u> <u>LEVEL</u>	<u>PRE-IMPACT</u>		<u>POST-IMPACT</u>		$\mu_2 - \mu_1$	<u>SIGNIFICANCE</u>
	μ_1	σ_1	μ_2	σ_2		
20 G	3.514	0.015	3.545	0.014	0.031	P<0.0005
60 G	3.431	0.014	3.473	0.007	0.042	P<0.0005
80 G	3.457	0.011	3.516	0.012	0.059	P<0.0005
100 G	3.453	0.018	3.568	0.111	0.111	P<0.0005

μ, σ - average and standard deviation, respectively,
of 58 latency estimates in milliseconds.

Significance - computed from one-tailed Student's-T, known and unequal variance.

B. Saltzberg, et al.

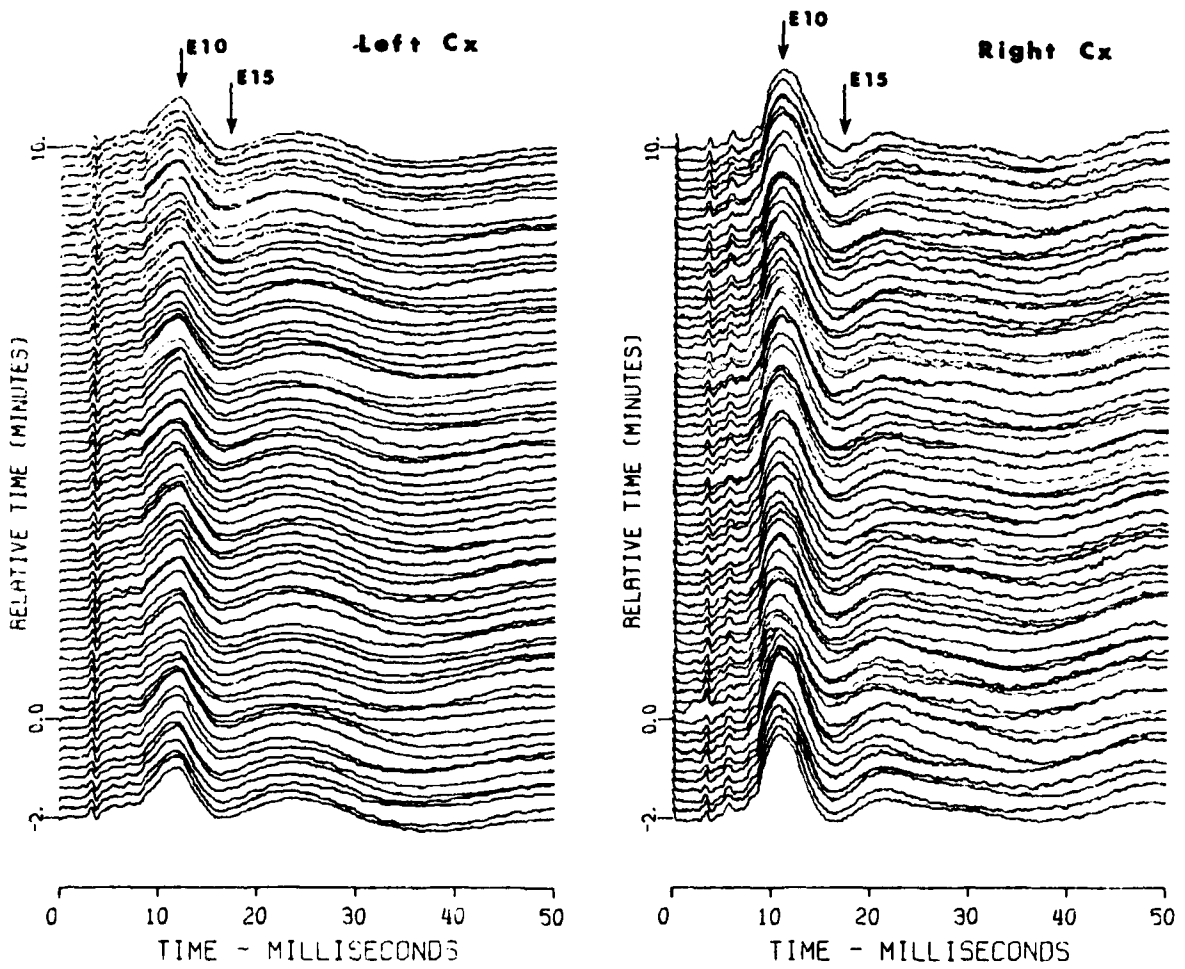


Figure 1. - AEP array plot for run LX-3469, 30G -Y. Each trace is the average of 50 responses.

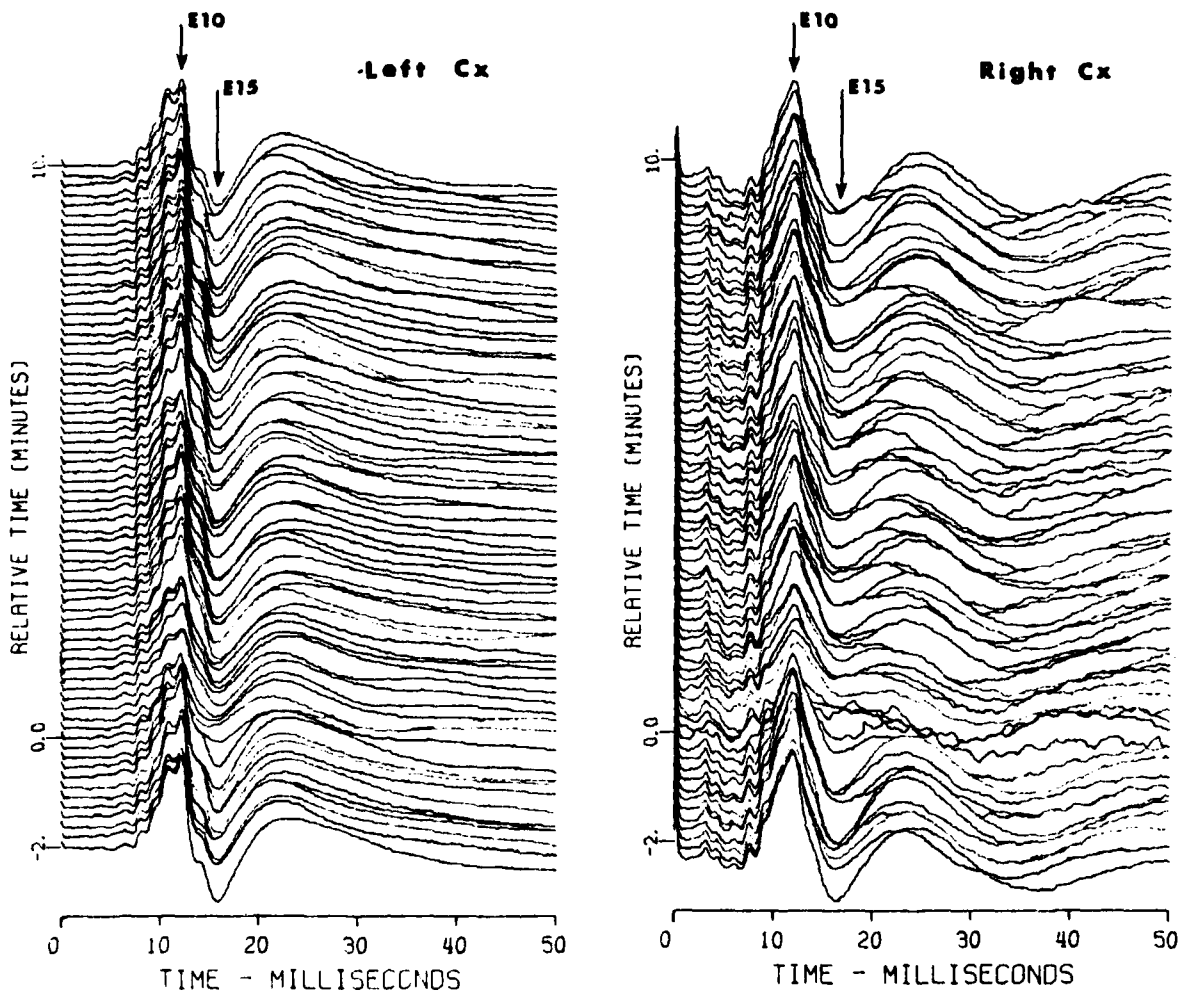


Figure 2. - AEP array plot for run LX-3473, 50G -Y. Each trace is the average of 50 responses.

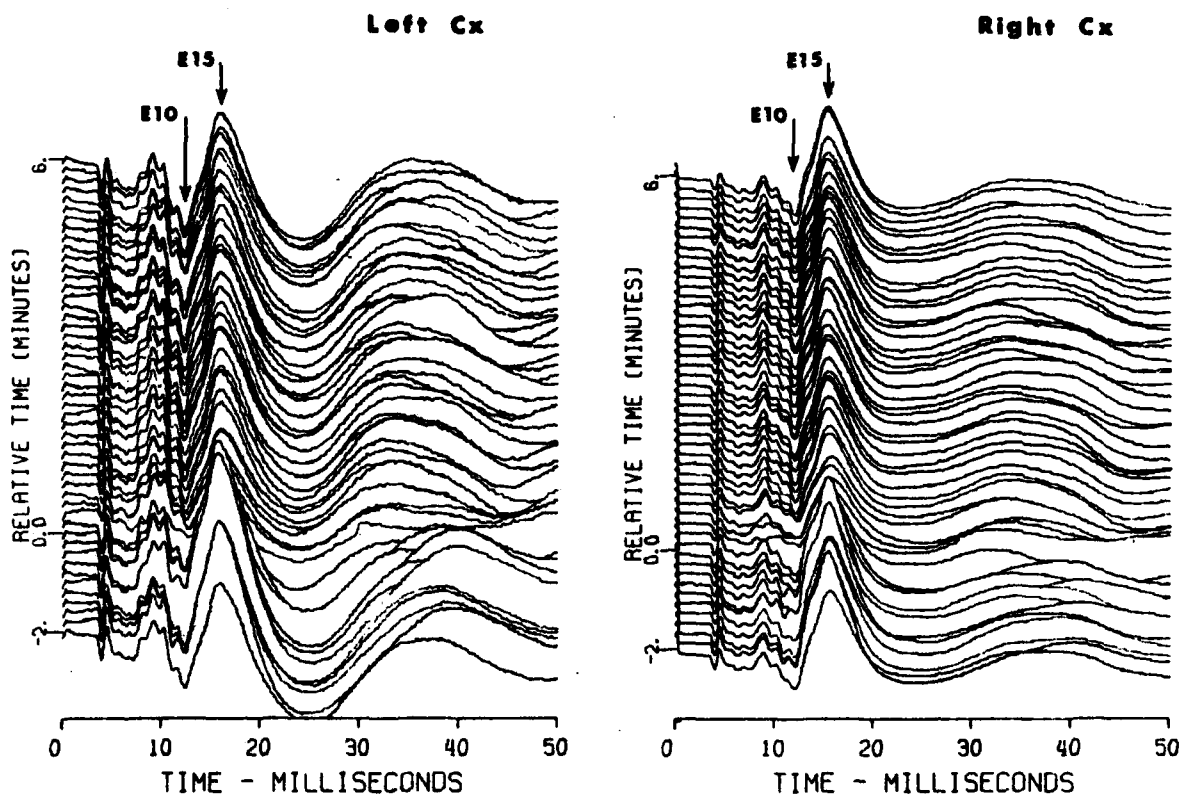


Figure 3. - AEP array plot for run LX-3471, 70 G -Y. Each trace is the average of 50 responses.

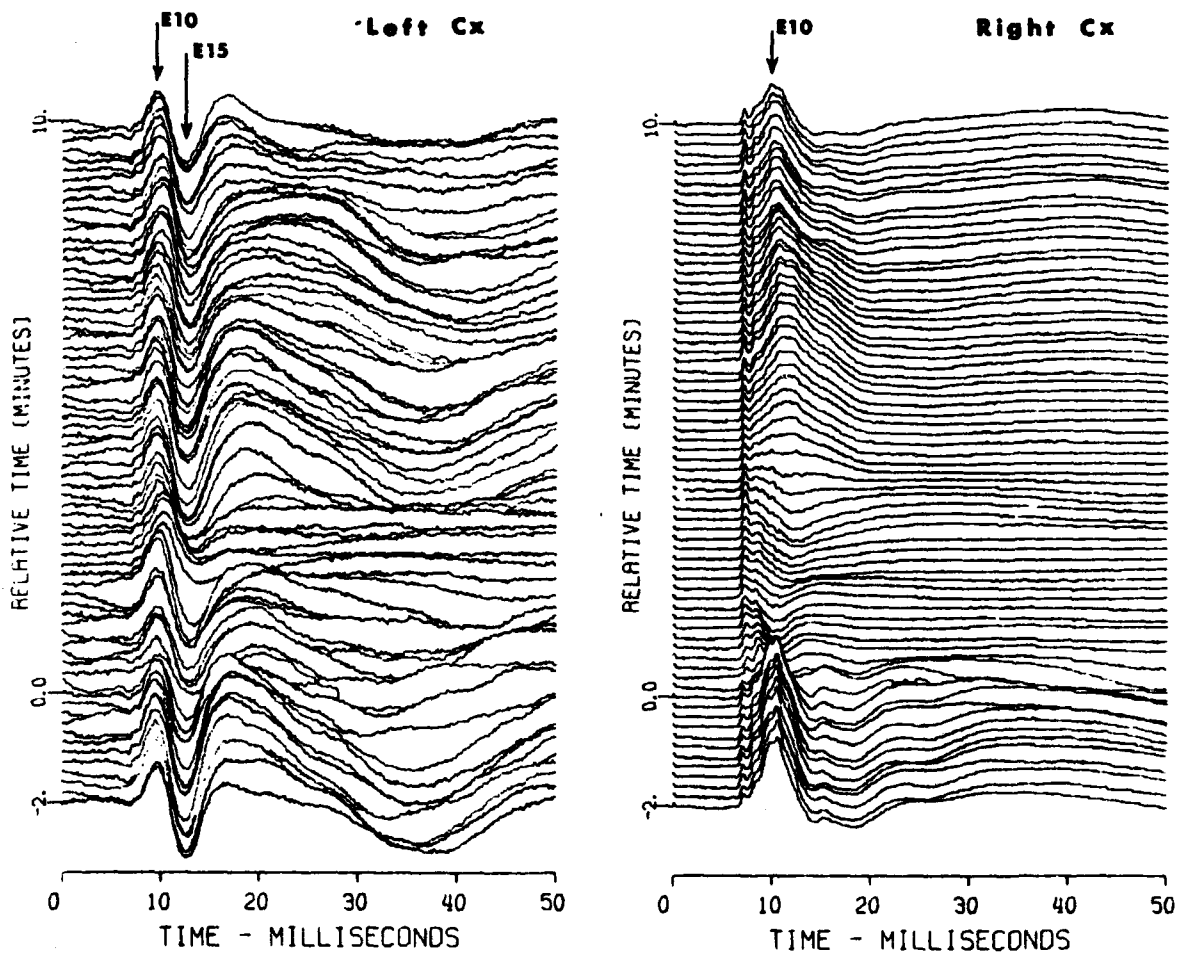
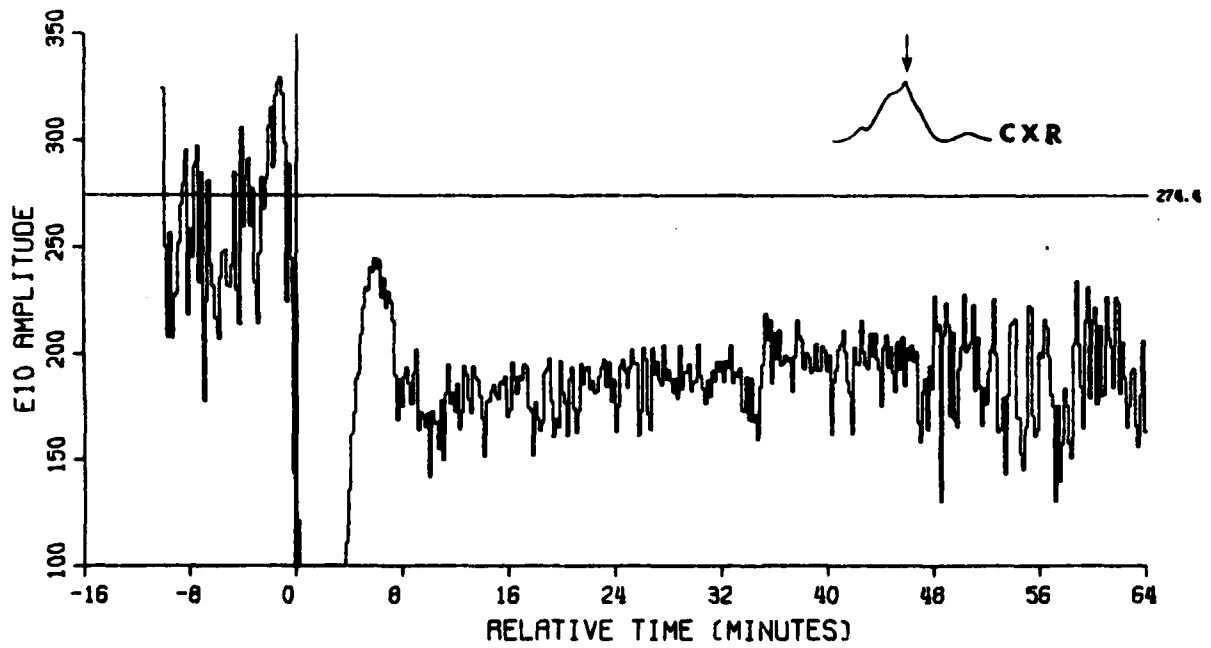
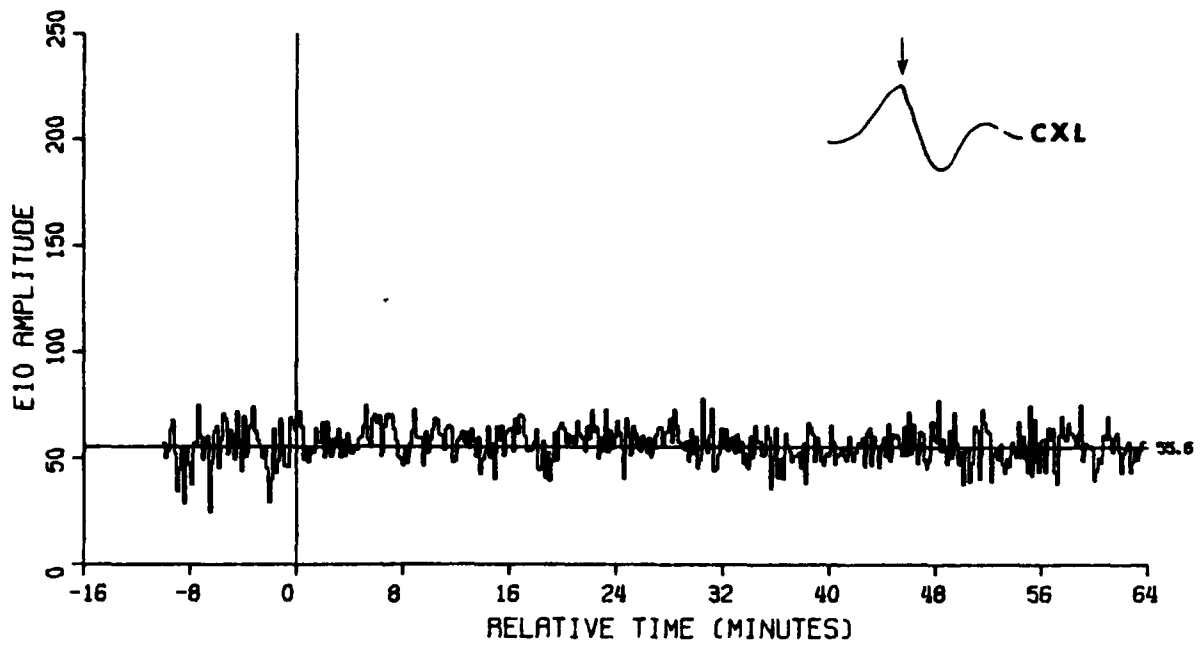


Figure 4. - AEP array plot for run LX-3475, 90 G -Y. Each trace is the average of 50 responses.

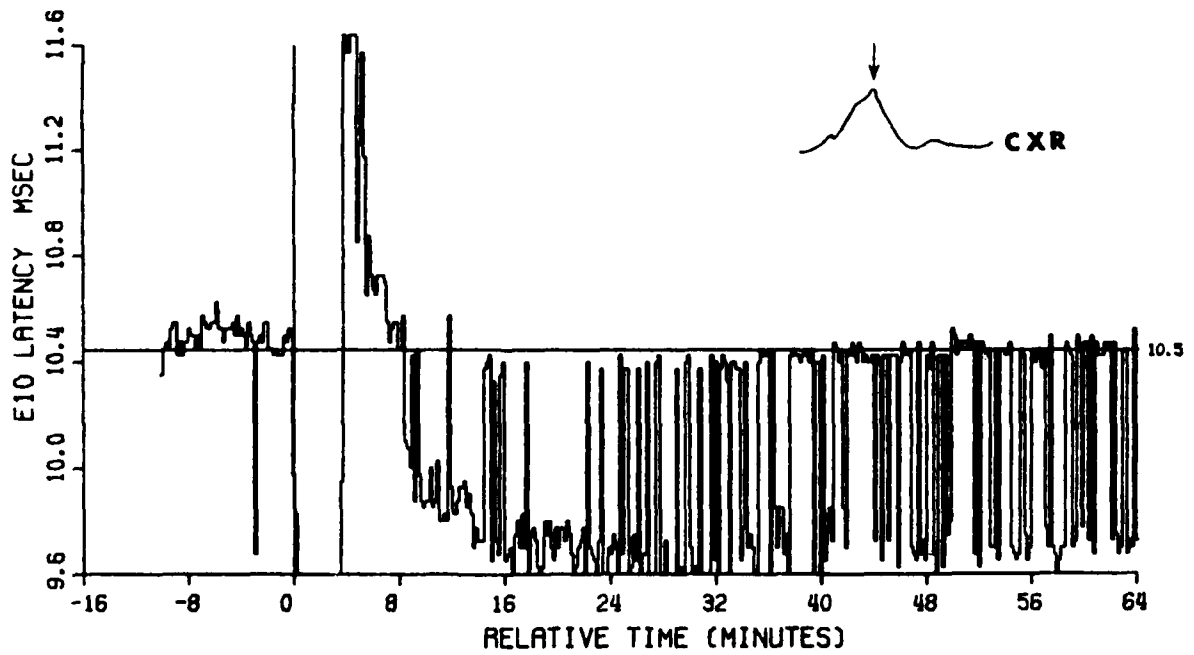
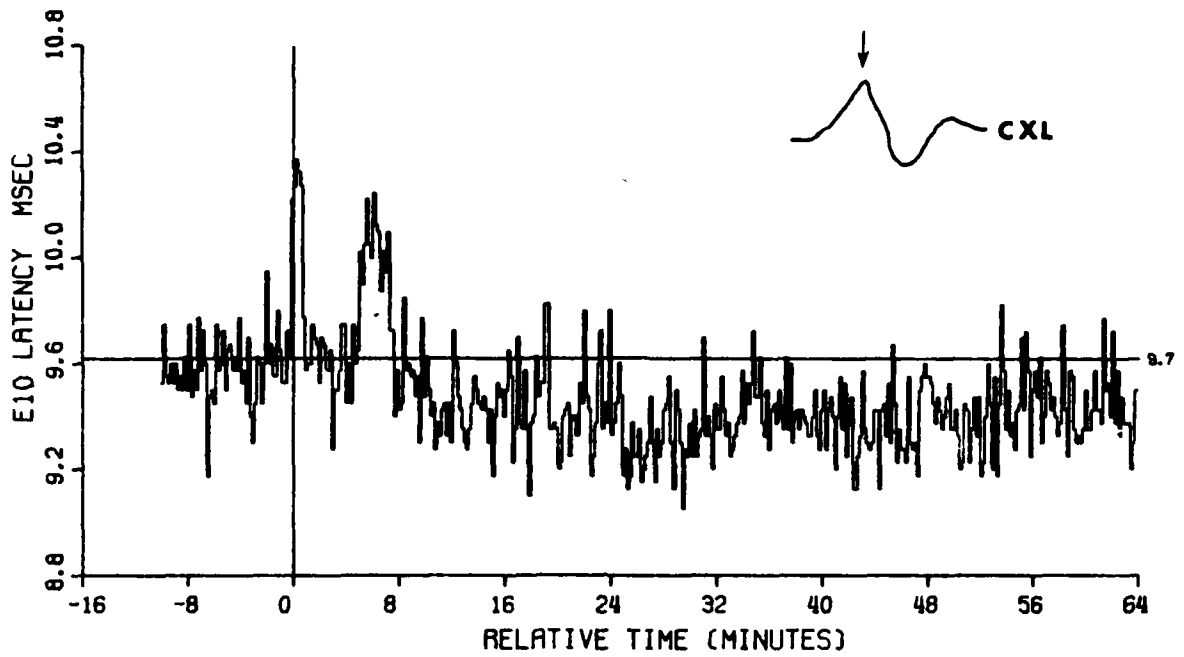


ANIMAL AA-0016
 STIMULUS SITE 7, SPINE
 RECORDING SITE 1, CXA

RUN LX-3475

ACCELERATION 90.0 G
 RATE 4.03 /SEC
 NBR. AVERAGED 50

Figure 5



ANIMAL AR-8816
 STIMULUS SITE 7, SPINE
 RECORDING SITE 1, CXR

RUN LX-3475

ACCELERATION 90.0 G
 RATE 4.83 /SEC
 NBR. AVERAGED 50

Figure 6

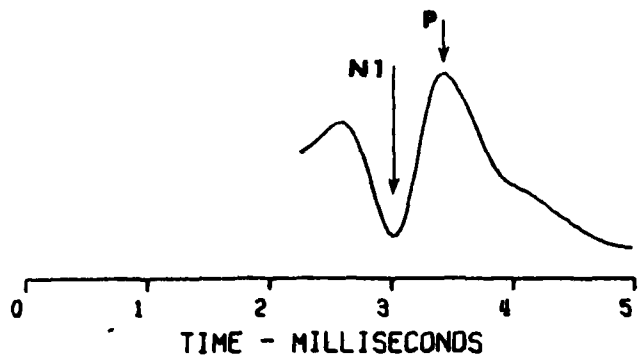


Figure 7. - Run LX-3015, Typical AEP response, sum of 20.

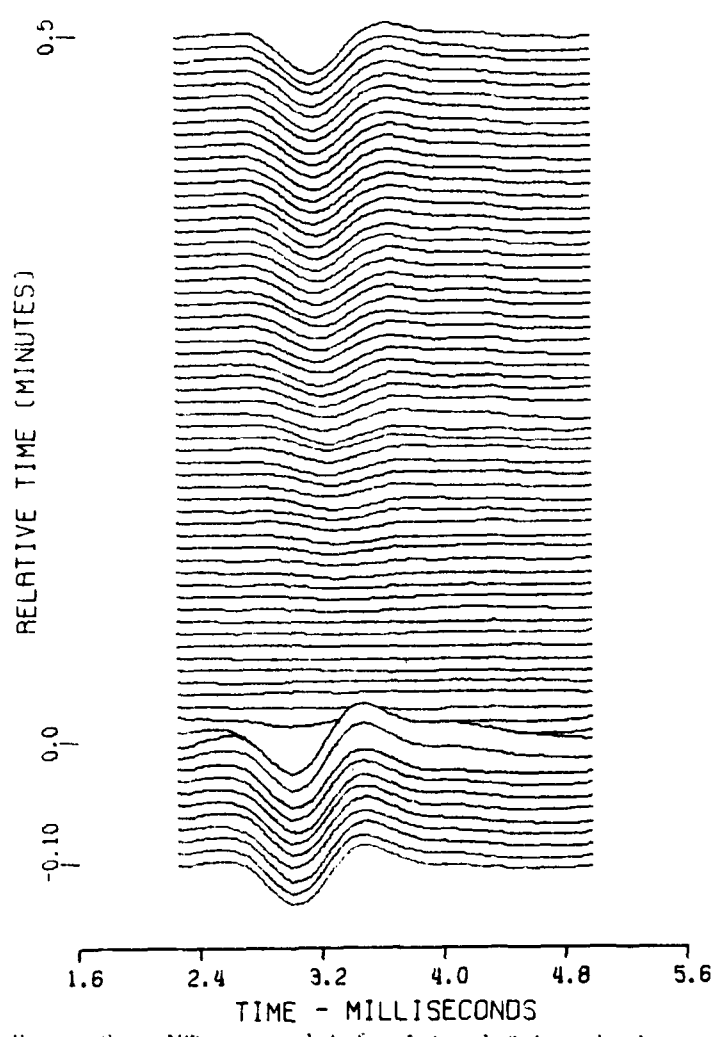
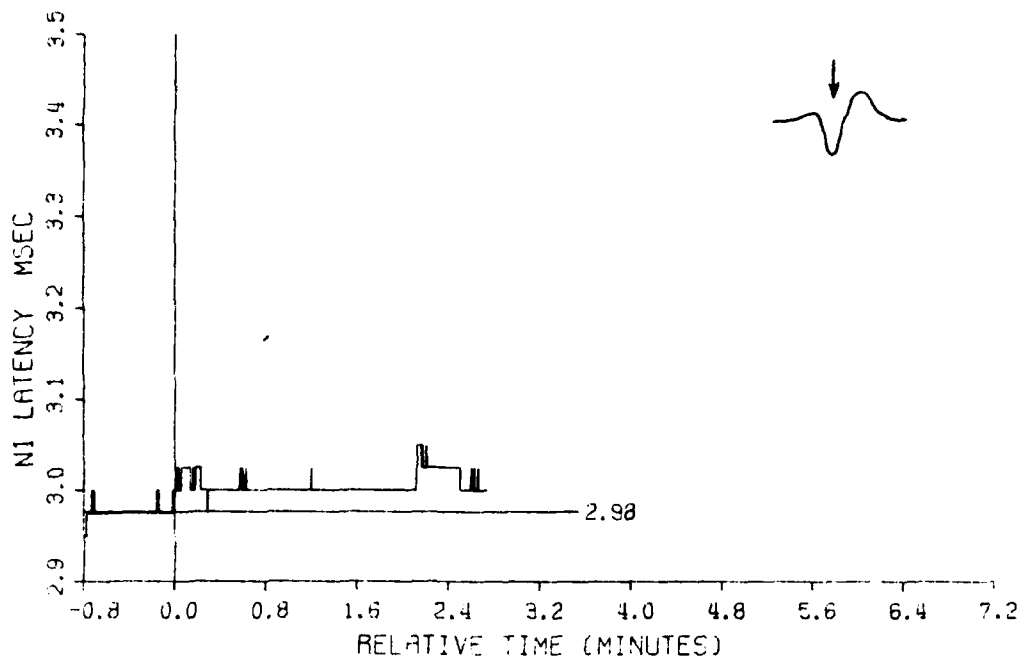
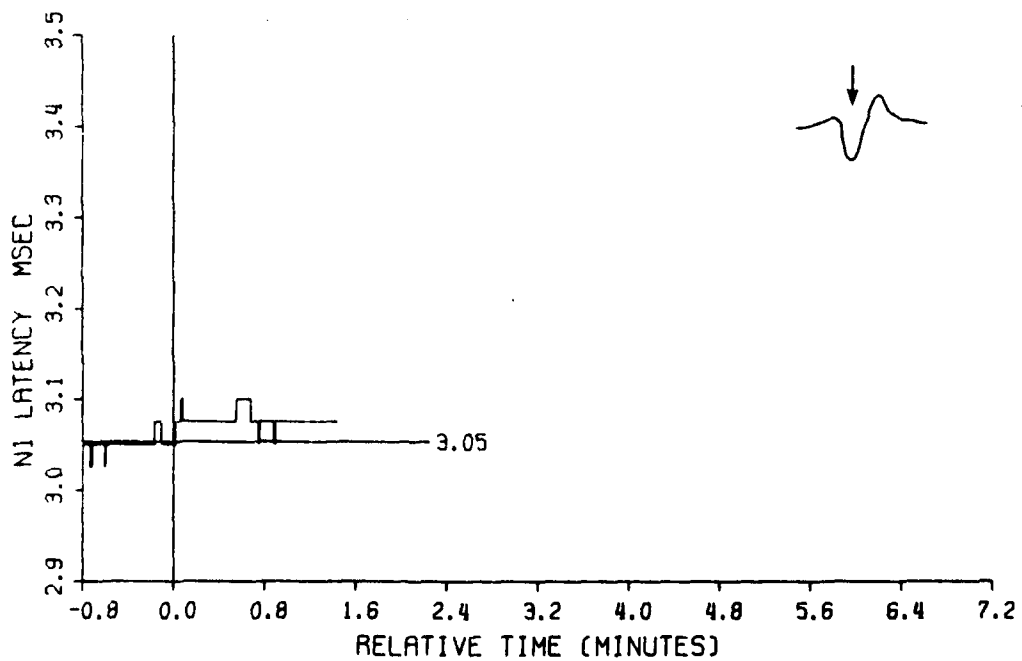


Figure 8. - AEP array plot for Lateral Column lead of run LX-3015, 100 G-X. Each trace is the average of 100 responses.



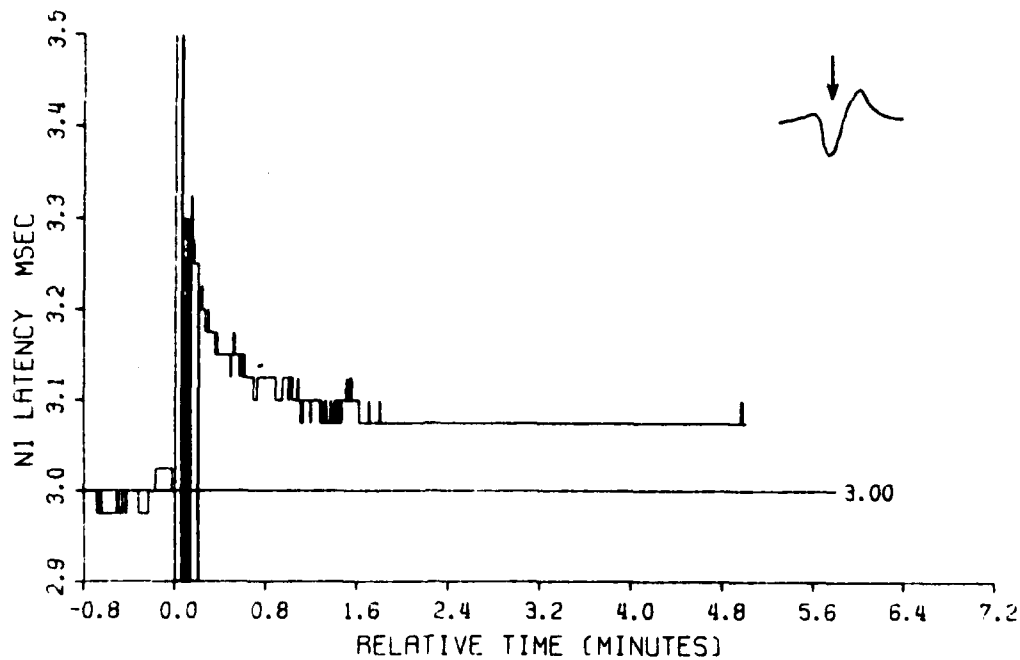
ANIMAL AR-0764 RUN LX-3013 ACCELERATION 50.0 G
 STIMULUS SITE 5, MOTOR CX RATE 191.56 /SEC
 RECORDING SITE 1, LAT COL NBR. AVERAGED 100

Figure 9



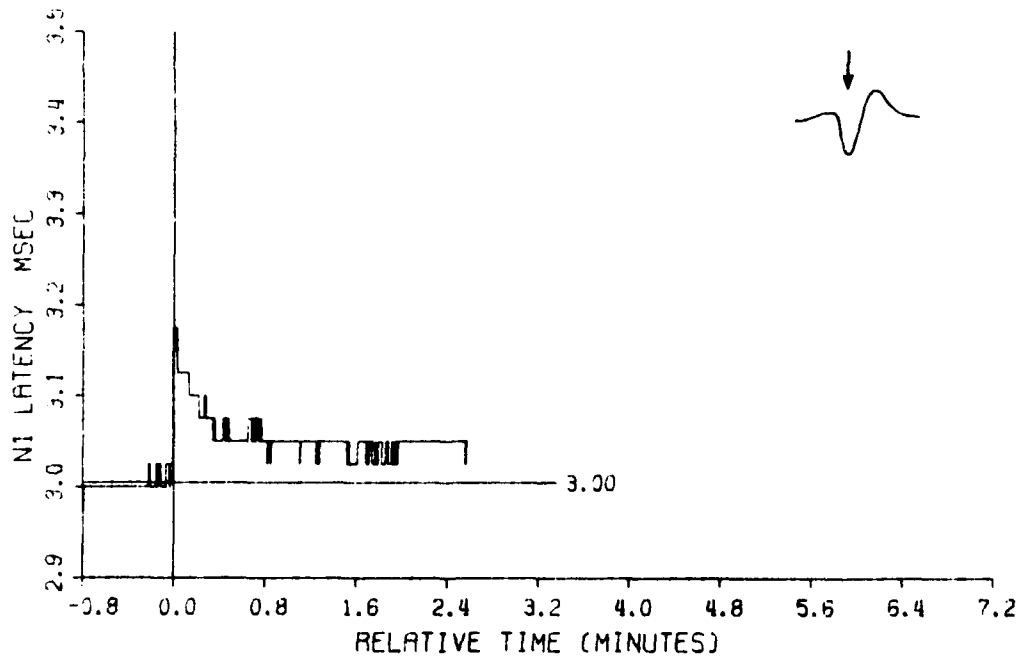
ANIMAL AR-0764 RUN LX-3012 ACCELERATION 20.0 G
 STIMULUS SITE 5, MOTOR CX RATE 191.71 /SEC
 RECORDING SITE 1, LAT COL NBR. AVERAGED 100

Figure 10



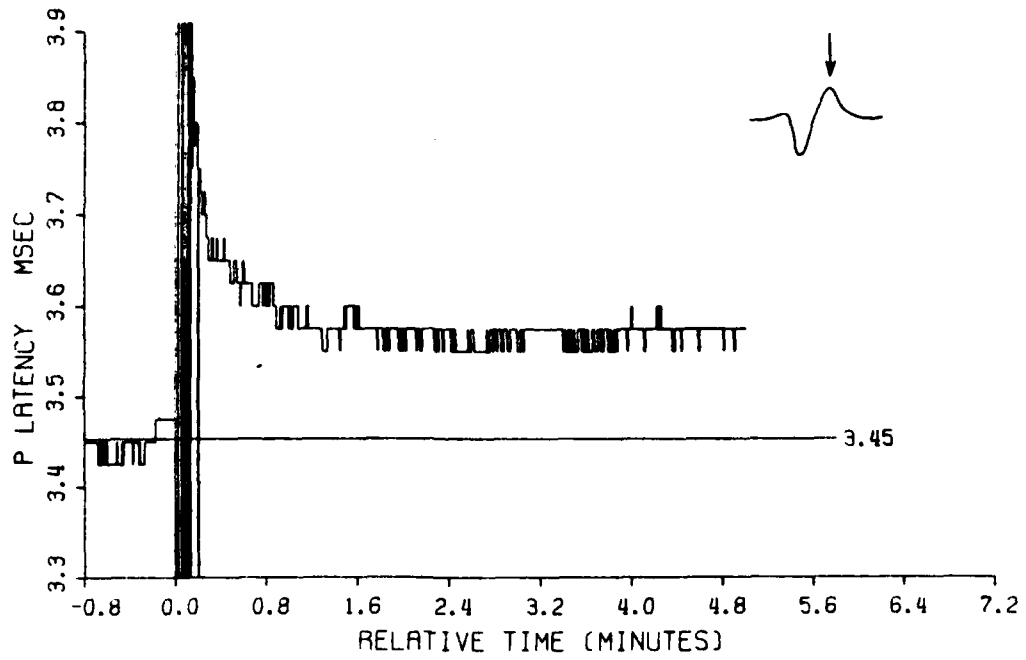
ANIMAL AA-0754 RUN LX-3015 ACCELERATION 100.0 G
 STIMULUS SITE 5, MOTOR CX RATE 191.47 /SEC
 RECORDING SITE 1, LAT COL NBA, AVERAGED 100

Figure 11



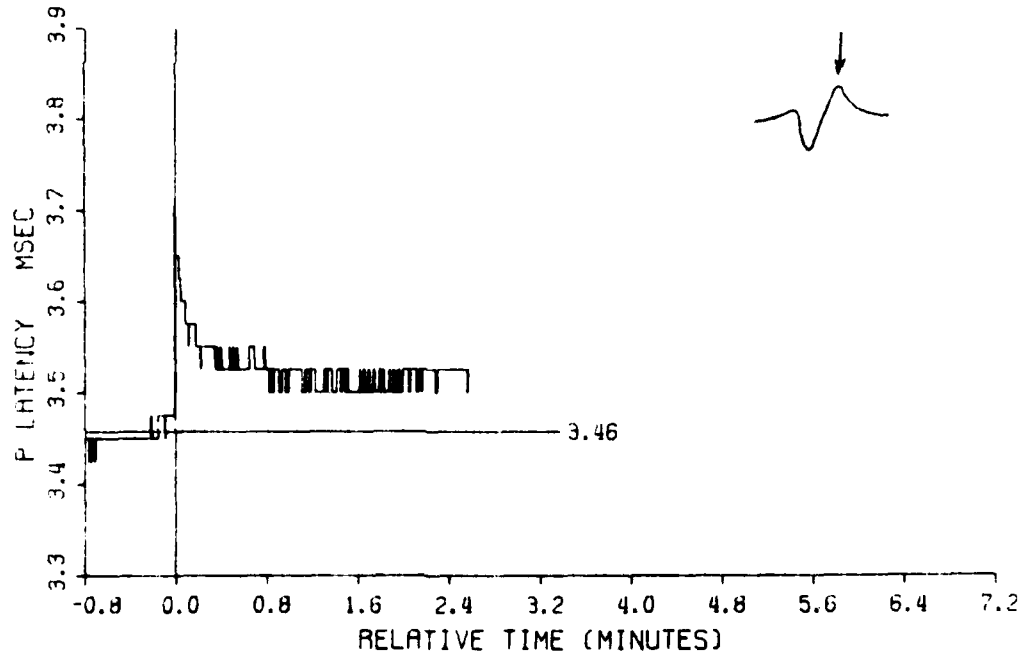
ANIMAL AA-0764 RUN LX-3014 ACCELERATION 80.0 G
 STIMULUS SITE 5, MOTOR CX RATE 191.50 /SEC
 RECORDING SITE 1, LAT COL NBA, AVERAGED 100

Figure 12



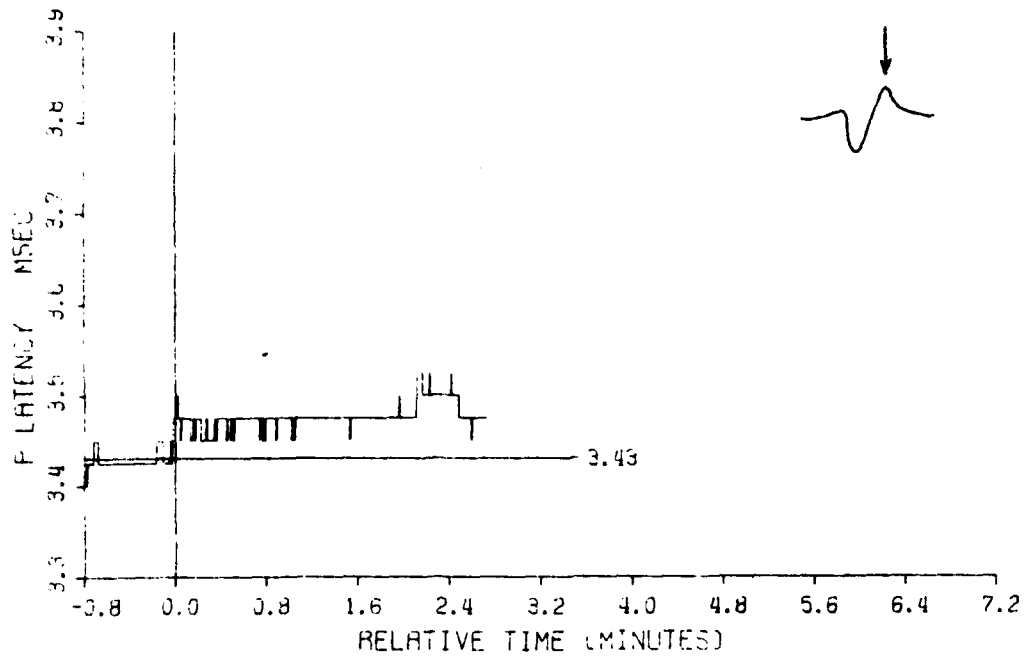
ANIMAL RA-0764 RUN LX-3015 ACCELERATION 100.0 G
 STIMULUS SITE 5. MOTOR CX RATE 191.47 /SEC
 RECORDING SITE 1. LAT COL NBR. AVERAGED 100

Figure 13



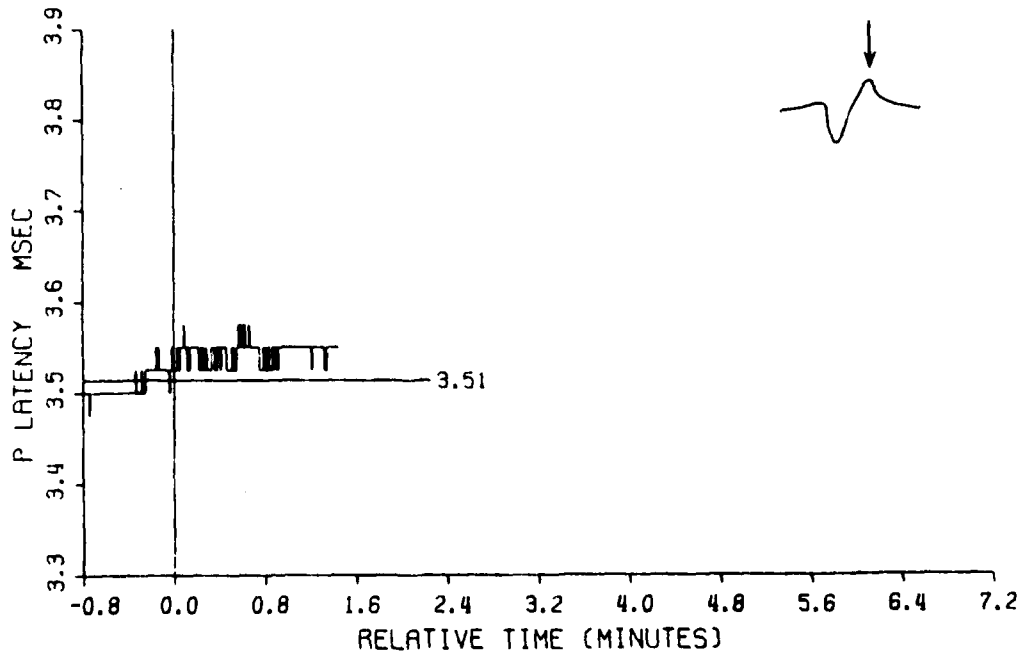
ANIMAL RA-0764 RUN LX-3014 ACCELERATION 80.0 G
 STIMULUS SITE 5. MOTOR CX RATE 191.50 /SEC
 RECORDING SITE 1. LAT COL NBR. AVERAGED 100

Figure 14



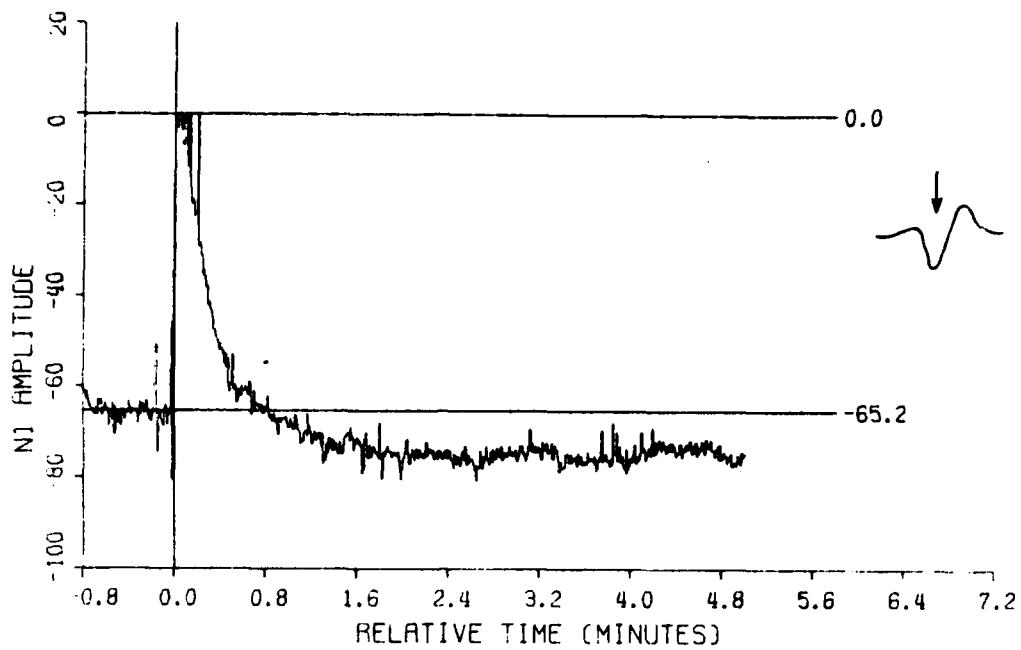
ANIMAL RA-0764 RUN LX-3013 ACCELERATION 60.0 G
 STIMULUS SITE S. MOTOR CX RATE 191.58 /SEC
 RECORDING SITE 1. LAT COL NBR. AVERAGED 100

Figure 15



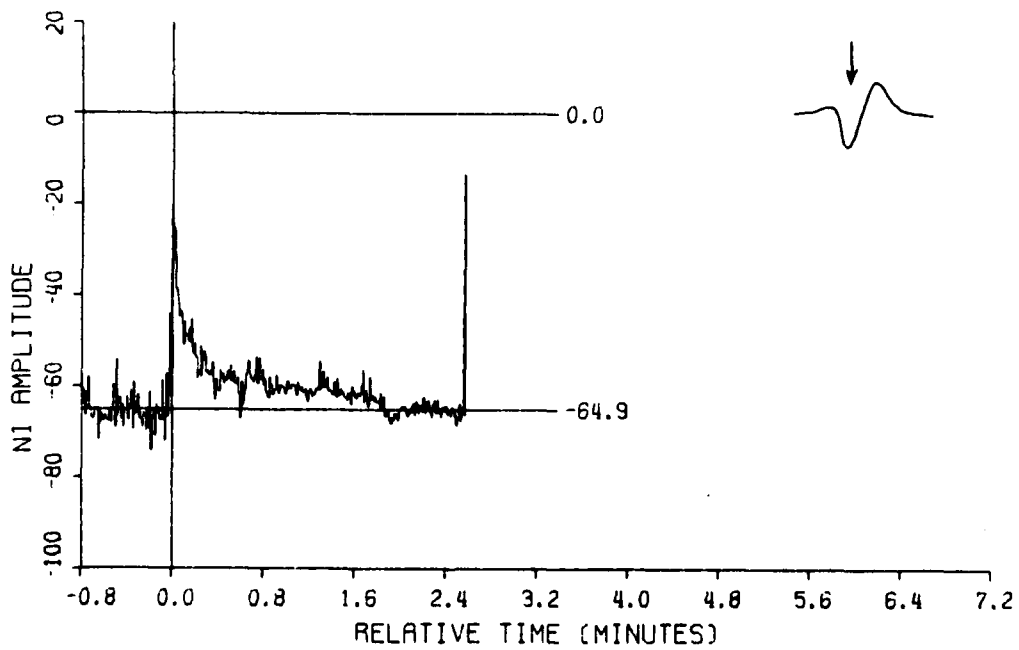
ANIMAL RA-0764 RUN LX-3012 ACCELERATION 20.0 G
 STIMULUS SITE S. MOTOR CX RATE 191.71 /SEC
 RECORDING SITE 1. LAT COL NBR. AVERAGED 100

Figure 16



ANIMAL AR-0764 RUN LX-3015 ACCELERATION 100.0 G
 STIMULUS SITE 5. MOTOR CX RATE 191.47 /SEC
 RECORDING SITE 1. LAT COL NBR. AVERAGED 100

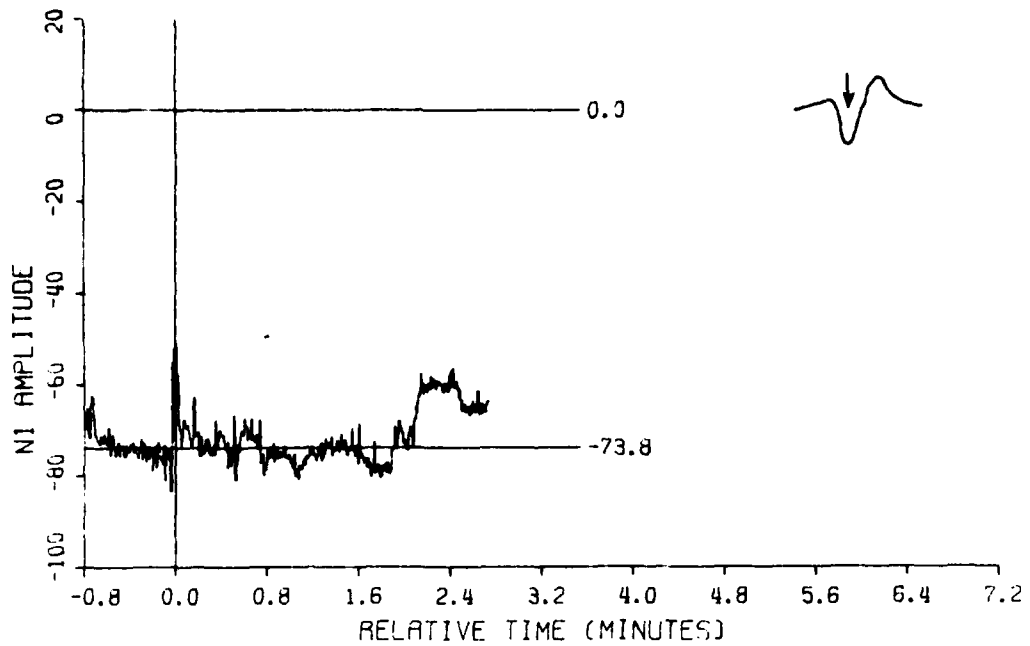
Figure 17



ANIMAL AR-0764 RUN LX-3014 ACCELERATION 80.0 G
 STIMULUS SITE 5. MOTOR CX RATE 191.50 /SEC
 RECORDING SITE 1. LAT COL NBR. AVERAGED 100

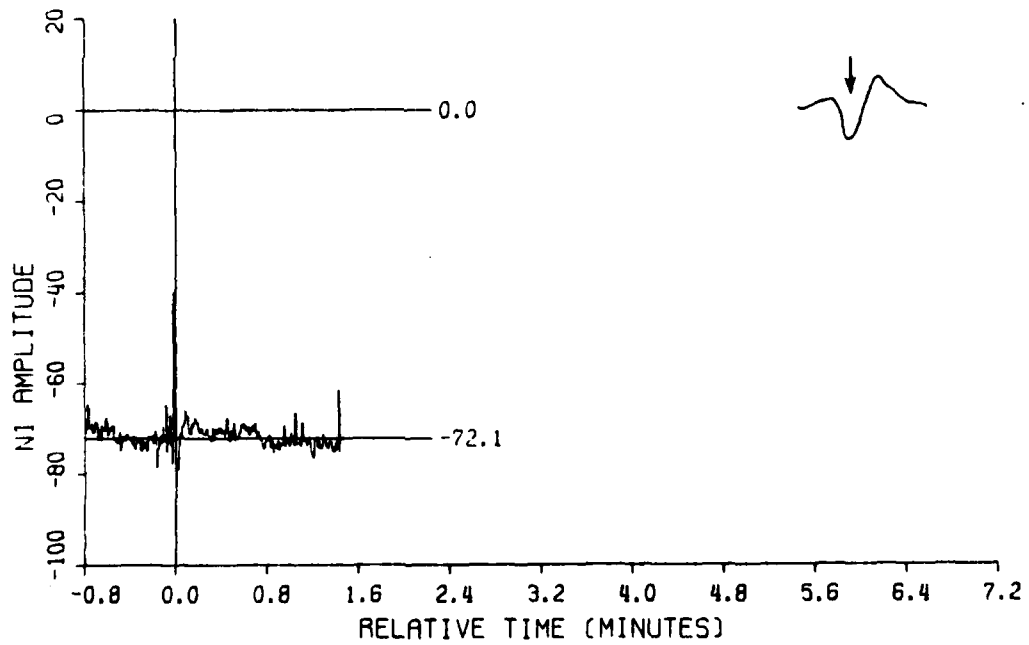
Figure 18

Saltzberg, et al.



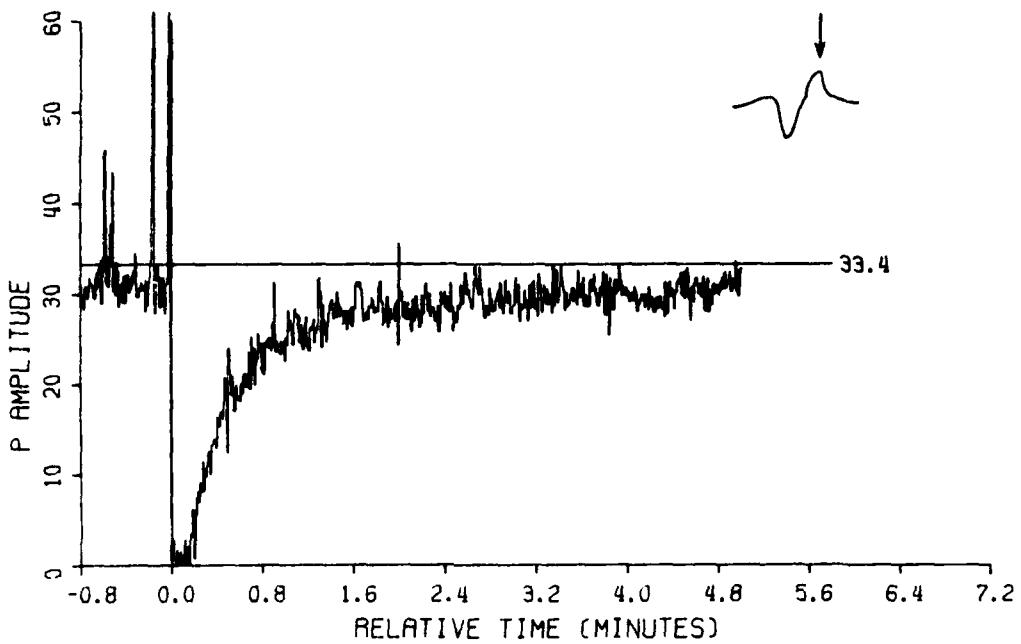
ANIMAL AR-0764 RUN LX-3013 ACCELERATION 60.0 G
 STIMULUS SITE 5. MOTOR CX RATE 191.56 /SEC
 RECORDING SITE 1. LAT COL NBA. AVERAGED 100

Figure 19



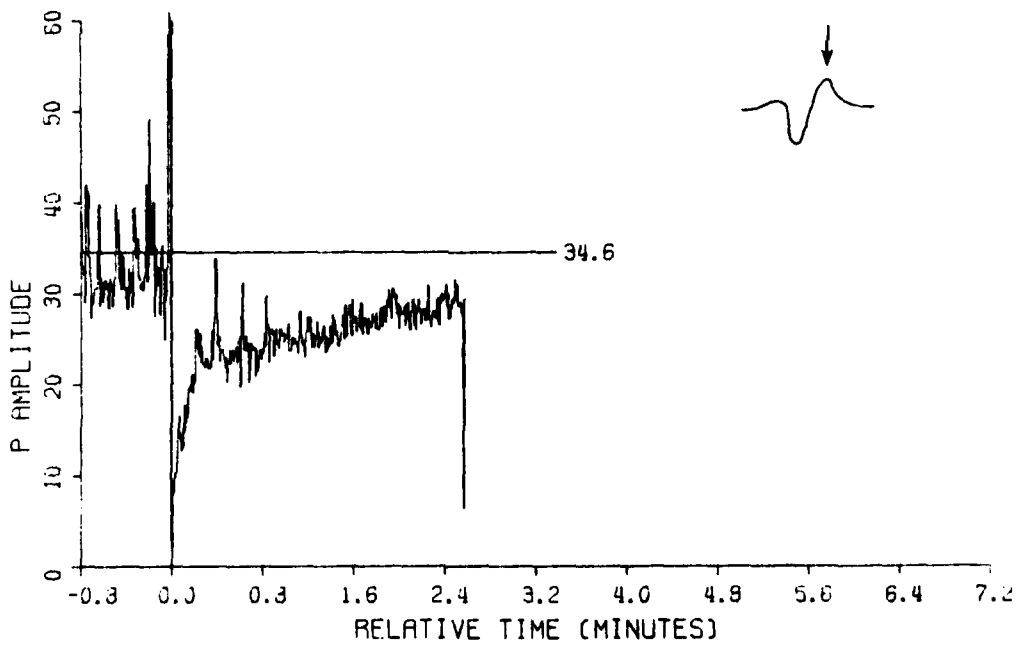
ANIMAL AR-0764 RUN LX-3012 ACCELERATION 20.0 G
 STIMULUS SITE 5. MOTOR CX RATE 191.71 /SEC
 RECORDING SITE 1. LAT COL NBA. AVERAGED 100

Figure 20



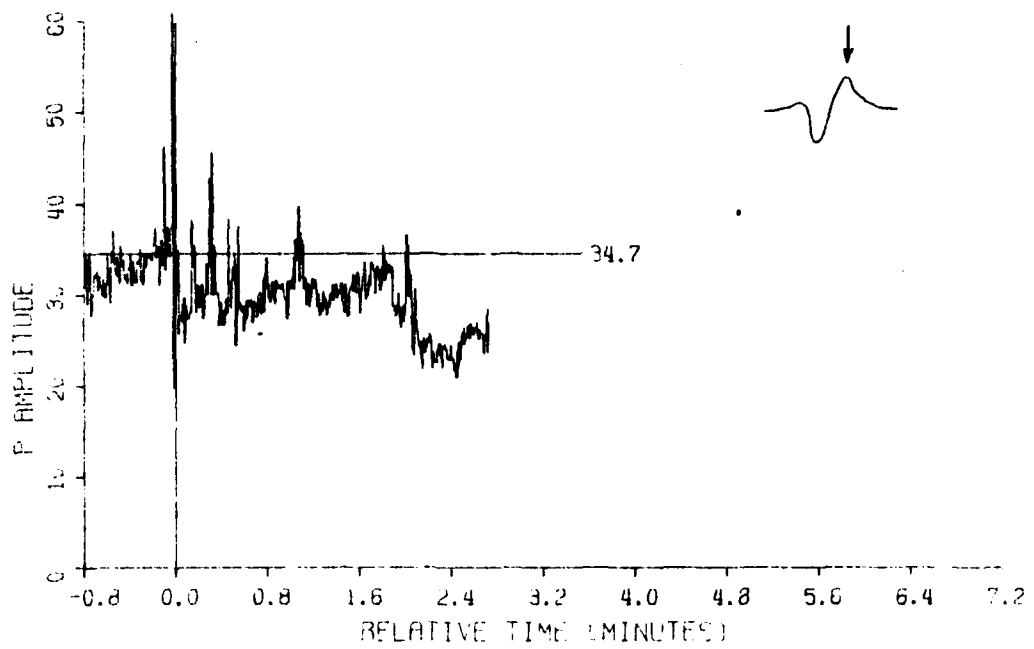
ANIMAL AR-0764 RUN LX-3015 ACCELERATION 100.0 G
 STIMULUS SITE 5. MOTOR CX RATE 191.47 /SEC
 RECORDING SITE 1. LAT COL NBA. AVERAGED 100

Figure 21



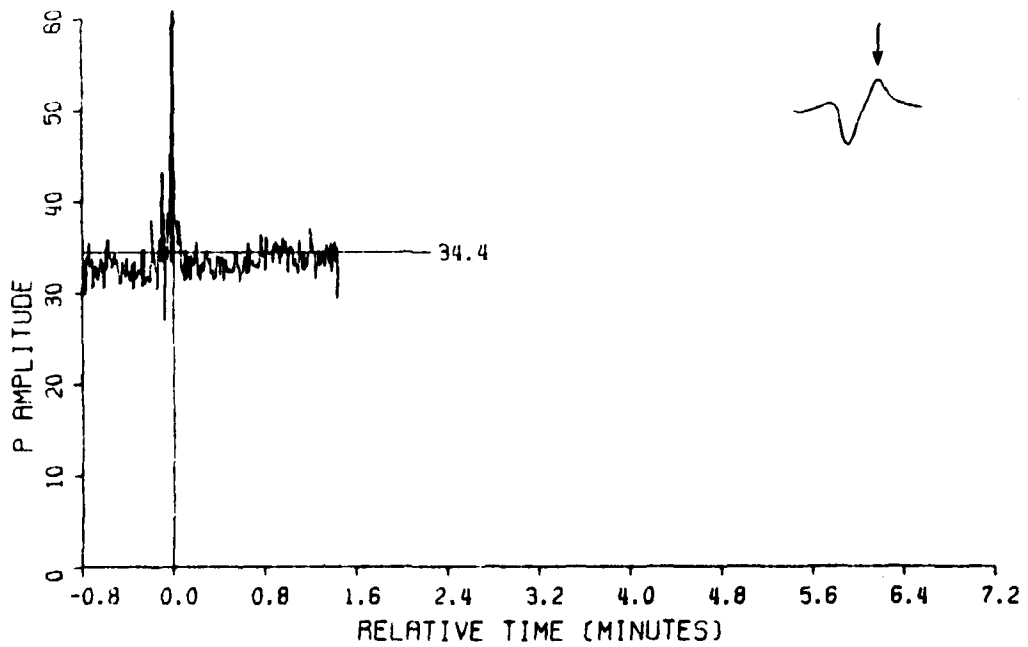
ANIMAL AR-0764 RUN LX-3014 ACCELERATION 80.0 G
 STIMULUS SITE 5. MOTOR CX RATE 191.50 /SEC
 RECORDING SITE 1. LAT COL NBA. AVERAGED 100

Figure 22



ANIMAL: AR-0064 RUN LX-3013 ACCELERATION 60.0 G
 STIMULUS SITE 5, MOTOR CX RATE 191.56 /SEC
 RECORDING SITE 1, LAT COL NBR. AVERAGED 100

Figure 23



ANIMAL AR-0064 RUN LX-3012 ACCELERATION 20.0 G
 STIMULUS SITE 5, MOTOR CX RATE 191.71 /SEC
 RECORDING SITE 1, LAT COL NBR. AVERAGED 100

Figure 24